N79 21498

Interpretation of Altimeter Data

Micheline C. Roufosse
Harvard-Smithsonian Center for Astrophysics
Cambridge, Massachusetts 02138

Abstract. Two methods are used to interpret the whole range of signals contained in the Geos 3 altimeter data. They each address a different class of events and thus complement each other in their ability to provide information on the state of convection in the earth's mantle. The long wavelength section of the spectrum yields information on the depth of the convection cells and the viscosity variations inside those cells through a study of the variations of the admittance as a function of wavelength. The short wavelength section of the spectrum provides information on the time evolution of the lithosphere, considered as a thin elastic plate, by studying its response to loads at several points in its evolution. The variation of the flexural rigidity with age is obtained from that study.

Introduction

The geoid heights derived from the Geos 3 experiment contain signals covering a whole spectrum of wavelengths that are related to various processes. It is thus useful to separate the whole spectrum into two large classes: short wavelength that covers signals smaller than 500 to 1000 km width and large wavelength that includes signals of larger width. These two ranges of wavelengths must be handled separately; their different origins require different methods of interpretation. The overall problem addressed by both methods is to characterize convection in the earth's mantle by use of two complementary approaches.

Long Wavelength Study

The central idea of the long wave study was developed by McKenzie and his coworkers in a series of numerical studies on convective flow [McKenzie, Roberts, and Weiss, 1974; McKenzie and Weiss, 1975; McKenzie, 1977]. Several two-dimensional models with different parameters were studied in order to determine how they affect the state of convection in the earth's mantle and how they relate to the observed quantities accessible to geophysicists. The result of this analysis is that the most relevant quantity to study is the behavior of the admittance as a function of wavelength; the admittance is defined as the ratio, in wavenumber space, of the gravity to the bathymetry.

The study of a wide range of numerical models shows that the admittance is insensitive to the Rayleigh number and the degree of internal heating but is strongly affected by viscosity variations and the depth of the convecting layer or the deformability of the lower boundary. So far, very little information has been available on the variation of the admittance with wavelength in oceanic regions as a result of inadequate gravity data coverage. Data collected over oceanic regions during the Geos 3 mission have solved that problem; and currently, adequate geoid height data are available over most oceanic regions. It is thus possible to derive the gravity field directly on the geoid by combining radar altimeter data, range-rate residuals, and surface ship observations. Each of the three sets of data must be written into a coherent network that reduces crossing errors to a minimum. Deriving the gravity field is then a linear inversion problem, which can be treated by any standard method. The Backus-Gilbert method, however, offers the advantage that both the gravity field and an estimate of its error as a function of latitude and longitude are obtained directly. Both bathymetry and gravity must then be Fourier-transformed into wavenumber space and divided by one another to give the admittance as a function of wavelength. This study will put more definite constraints on the lower boundary and viscosity variations characterizing convection in the mantle.

Short Wavelength Study

The short wavelength signals in the geoid heights yield information on the time behavior of the lithosphere. Following Crough [1975], we can consider the lithosphere as a thin plate whose thickness increases with increasing time up to a certain age, of the order of 80 m.y., and then continues to increase at a progressively lower rate until it reaches equilibrium thickness. Since the thickness of a plate influences its mechanical properties, it is possible to study the time evolution of the lithosphere by observing how it deforms when loaded by seamounts placed at several points along its evolutionary path. To examine the mechanical properties of the lithosphere, we assumed the thin-plate model developed by McKenzie and Bowin [1976]. In this model, the lithosphere consists of a thin elastic plate overlying a fluid medium; the plate is being loaded by bathymetric features such as seamounts, island chains, and ridges and is subsequently deformed. The magnitude and wavelength of the deformed area depend mostly on the flexural rigidity, which is proportional to the cube of the lithospheric thickness. By studying the correlation function between the geoid height and the bathymetry, we can determine the flexural rigidity of the area under investigation. This can be done in one of two ways: the first is to Fourier-transform the geoid height and the bathymetry into wavenumber space, divide the geoid height by the bathymetry, and obtain the response function as a function of wavelength; the flexural rigidity can then be deduced from the characteristics of this function. The second method is to calculate a theoretical filter $Z(k)$ in wavenumber space by using the thin-plate model [McKenzie and Bowin, 1976] and varying the values for the

Proc. of the 9th GEOP Conference, *An International Symposium on the Applications of Geodesy to Geodynamics, October 2-5, 1978.* Dept. of Geodetic Science Rept. No. 280, The Ohio State Univ., Columbus, Ohio 43210.

flexural rigidity:

$$Z(k) = \frac{3(\rho_c - \rho_w)}{2r\rho_e \gamma} \frac{(1 - e^{-wkt})\ e^{-wkd}}{[1 + (wk)^4]\ wk} \quad (1)$$

where

$$\gamma = \left[\frac{(\rho_m - \rho_c)}{F}\right]^{1/4} \quad (2)$$

$$w = \frac{2\pi}{n\Delta\gamma} \quad (3)$$

In these expressions, ρ_c, ρ_w, ρ_m, and ρ_e are, respectively, the crustal, water, mantle, and mean-earth densities, r is the earth's equatorial radius, t is the crustal thickness, d is the water depth, g is the average gravity, F is the flexural rigidity, n is the number of points in the filter, and Δ is the spacing between consecutive points of the filter. The filter derived in equation (1) is then Fourier-transformed into direct space and convolved with the bathymetry, resulting in a theoretical geoid height. The value for the flexural rigidity that gives the best agreement between predicted and observed geoid heights is the one that will be selected for each area studied.

In practice, the method chosen will depend on the type of data available. The first method is more adequate when comparing gravity and bathymetry data from surface ships because both sets of data give equispaced points and can thus be easily Fourier-transformed. The second method, however, is preferable when dealing with Geos 3 altimeter data because it is not dependent on having both bathymetry and geoid-height data in a Fourier-transformable format. The Geos 3 data are easily transformed, but the bathymetry data must be reconstructed, as rigorously as possible, along the subsatellite position by using bathymetric contour charts; this operation generally results in poor accuracy and irregular point spacing. The second method, the two-dimensional approach, is thus the one we have used to study the evolution of the lithosphere. The regions

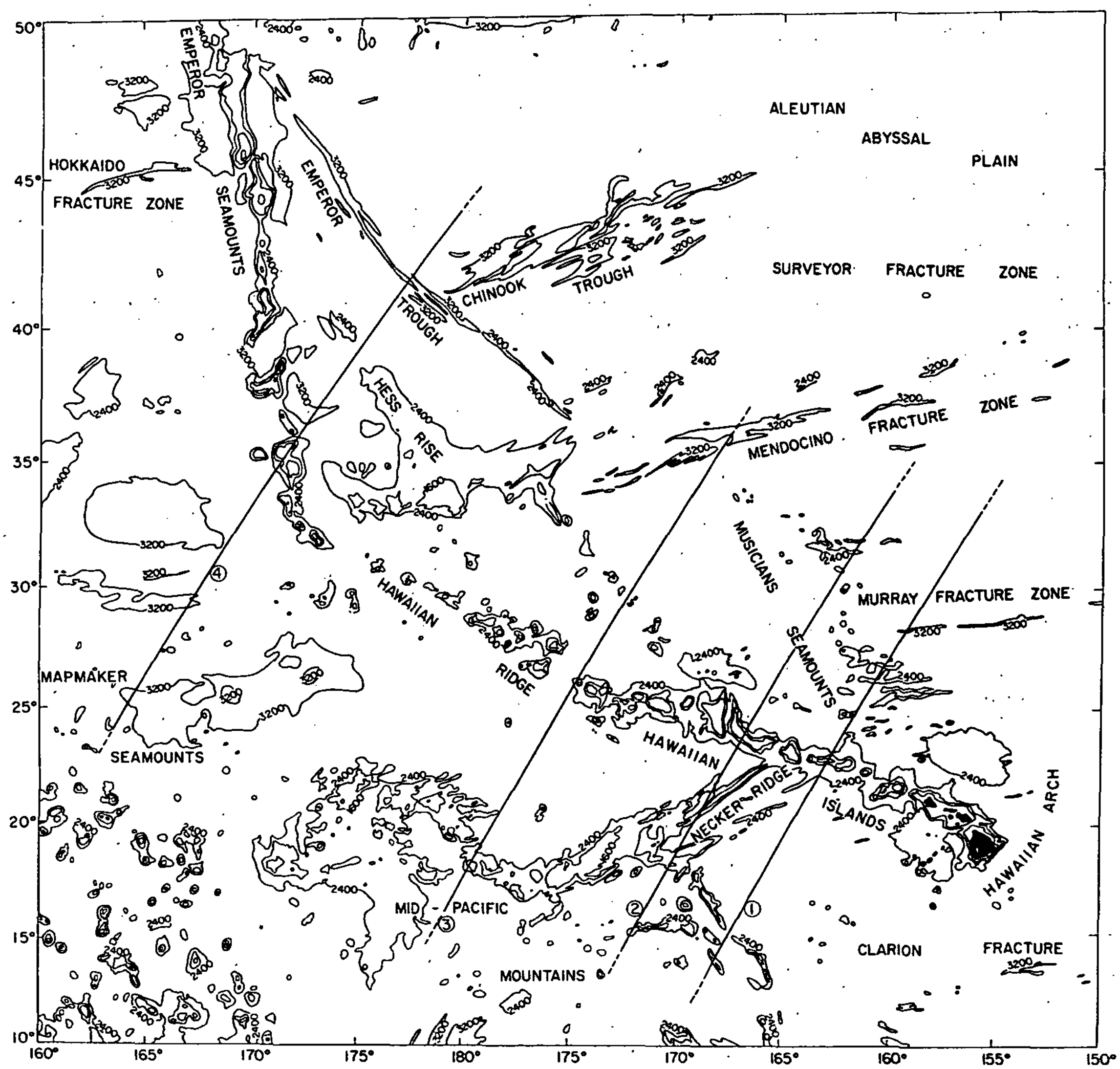

Fig. 1. Geos 3 passes studied in the Hawaiian-Emperor Seamounts region.

C-4

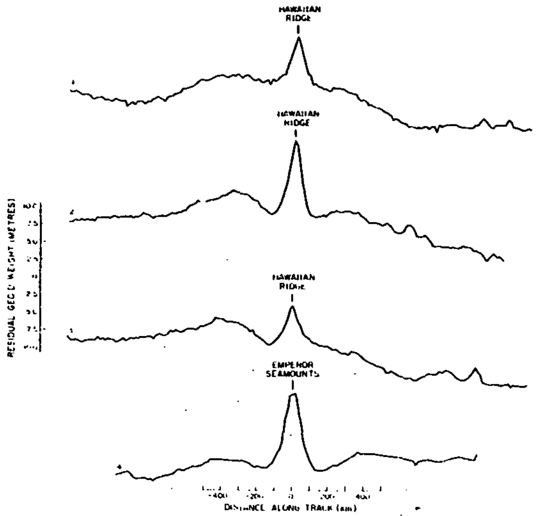

Fig. 2. Observed geoid height profiles in the Hawaiian-Emperor Seamounts region, represented with respect to a reference geoid of degree and order 12.

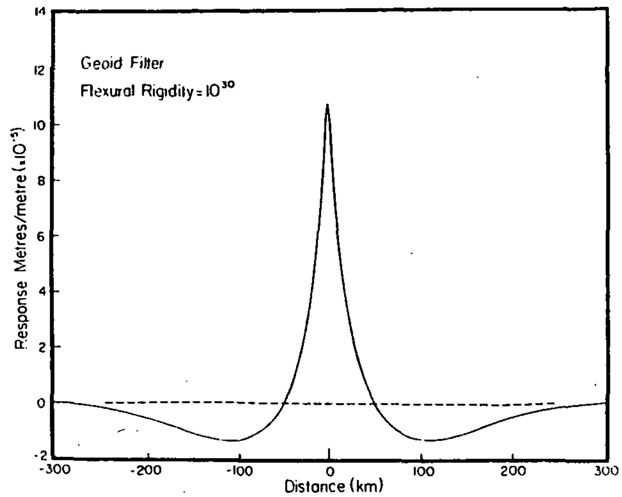

Fig. 3. Theoretical geoid filter calculated with a flexural rigidity of 10^{30} dyne cm.

studied so far are the Hawaiian-Emperor Seamount chain, the Marshall-Gilbert Island chain, and the Crozet Islands; these areas will be part of a much larger network.

The Hawaiian-Emperor Seamounts were selected first because they have been previously studied by other methods from other sets of data [Watts and Cochran, 1974; Walcott, 1976]. This area therefore constitutes an ideal testing ground for the two-dimensional technique. The altimeter passes from Geos 3 selected in that area are superposed on a map of the region in Figure 1, and their profiles are shown in Figure 2. The profiles are represented with respect to a reference geoid of degree and order 12 calculated from Standard Earth IV spherical-harmonics coefficients; they all show the features typical of the region — a sharp peak centered on the island chain flanked by a shallow depression and superposed on an asymmetrical bulge.

We then calculated theoretical filters using values for flexural rigidity ranging from 10^{29} to 10^{31} dyne-cm; an example, with a flexural rigidity of 10^{30} dyne-cm, is represented in Figure 3. After convolving the filters with the reconstructed bathymetry, we got the results shown in Figure 4. The top profile in the figure is the observed geoid represented with respect to a reference geoid of degree and order 16, which was chosen in order to remove the unwanted long-wavelength features; the middle profile is the best-fitting predicted geoid, obtained with a value of 10^{30} dyne-cm for the flexural rigidity; and the bottom profile is the bathymetry reconstructed along the subsatellite positions from the bathymetric charts designed at Scripps Institute of Oceanography by Chase, Menard, and Mammerickx [1970]. Our values for all passes are in close agreement with those determined by other methods [Watts and Cochran, 1974; Suyenaga, 1977].

In the framework of the time evolution of the lithosphere, two important observations were made in that region:

1. Predictions for the mid-Pacific Mountains are best when a lower value for flexural rigidity is used. This is in quantitative agreement with a study by Larson [1976] on the evolution of the Western Central Pacific Ocean. Interpreting the magnetic anomalies, he characterized the mid-Pacific Mountains as a slowly spreading center. A reduced plate thickness would thus be expected, as observed in the present work.

2. The flexural rigidity associated with the Emperor Seamounts is somewhat smaller then the easternmost active volcanoes of the Hawaiian chain, as shown in Figure 5; it is on the order of 8×10^{29} dyne-cm. The smaller value can be explained by taking into account the age of the seamounts along the chain [Clague and Jarrard, 1973]. In a recent study, Watts [1978] observed the correlation between gravity and bathymetry data obtained from surface ships over several sections of the Pacific Ocean: the East Pacific Rise, the Hawaiian-Emperor Seamounts, and the Kuril Rise. He deduced that the relevant factor related to flexural rigidity is the age of the lithosphere at the time of loading. Although the lithosphere in the case of the Emperor Seamounts is older than it is at the head of the Hawaiian chain, the load there is proportionally older, and therefore the lithosphere at the time of loading was younger, thus requiring a smaller flexural-rigidity value. So far, only one Geos 3 track is available for interpretation in that region; the difference observed is within the range of permissible uncertainties, but we cannot draw any definitive conclusions until more tracks along the seamount chain have been studied.

The two other areas investigated — the Marshall Gilbert Island and the Crozet Island — exhibited quite similar behavior to that found above. In the Geos 3 track shown crossing the Gilbert Islands chain in Figure 6, the top profile represents the bathymetry reconstructed from the Chase et al. chart, and the bottom profile is the

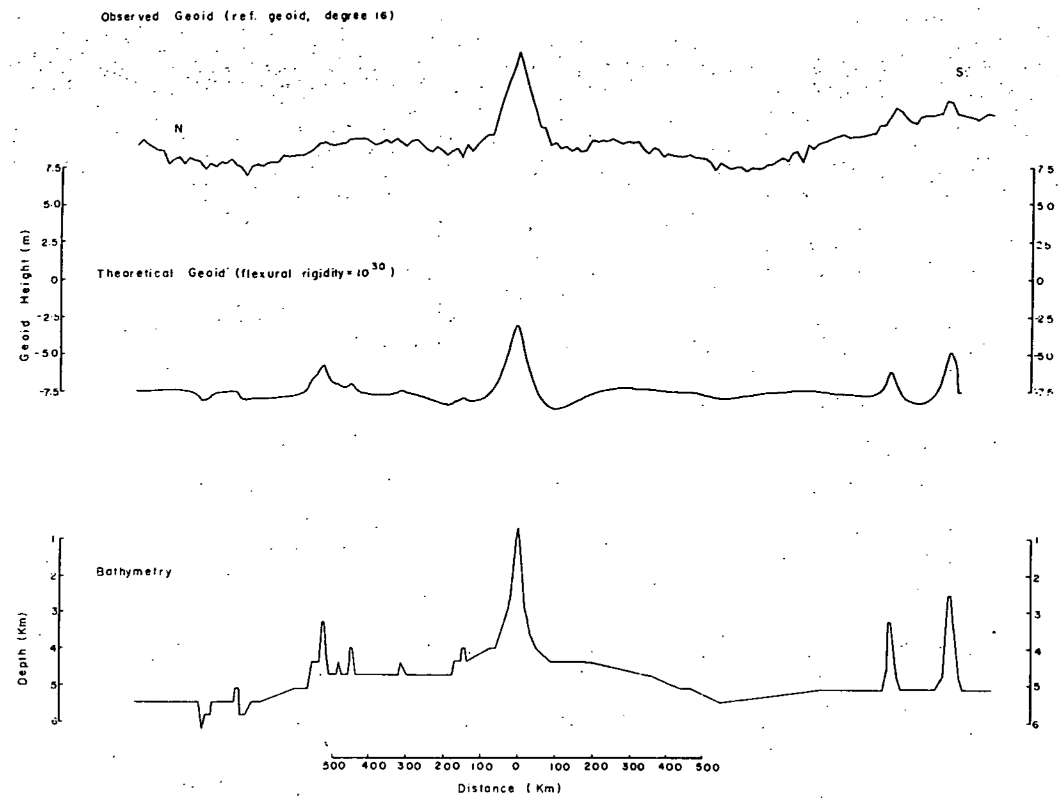

Fig. 4. The top profile represents the observed geoid height with respect to a reference geoid of degree and order 16 in the Hawaiian region; the intermediate profile is the predicted geoid, calculated with a filter of flexural rigidity of 10^{30} dyne-cm, and convolved with the bathymetry represented on the bottom profile.

observed geoid height with respect to a 16th-order reference geoid. The Gilbert Islands are the sharp feature seen at 1200 km. Figure 7 shows a series of predicted geoids in the same area computed with several values for flexural rigidity. Both the width and the height of the signal vary considerably, and the best-fitting value in this case is between 0.5 and 0.75 x 10^{30} dyne-cm. The lithosphere is quite old in that area, of the order of 120 m.y., and therefore a large lithospheric thickness is expected, which is inconsistent with the small value found for the flexural rigidity. To reconcile the present observation with Watt's model, it could be speculated that the Gilbert Islands constitute old loads.

The study of the Crozet Plateau was done in collaboration with Dr. Anny Cazenave, from Groupe de Recherche et de Geodesie Spatiale and Centre National d'Etudes Spatiales, Toulouse, who provided the relevant Geos 3 profiles. In a recent work, Cazenave and Lambeck (in preparation) analyzed the geoid anomalies in that region using the three-dimensional approach developed by Watts, Cochran, and Selzer [1975] for their study of the Great Meteor Seamount. Cazenave and Lambeck found that flexural-rigidity values ranging from 0.75 to 1 x 10^{30} dyne-cm gave an excellent fit between observed and predicted geoids. When we applied the two-dimensional approach described above to the Crozet Islands, we obtained a flexural-rigidity value similar to theirs; this can be seen by comparing the observed geoid plotted in Figure 8 and the predicted geoids shown in Figure 9.

In the Crozet Plateau region, the age of the load is unknown, and the age of the lithosphere, according to Schlich [1975], is Upper Cretaceous. A comparison of Cazenave and Lambeck's method with ours suggests that the two-dimensional approach is ideal for studying linear features such as island or seamount chains, while it offers less precision for dealing with individual features. In the case of the Crozet Plateau, only those tracks crossing the maximum altitude of the plateau gave a correct value for the flexural rigidity; all others resulted in larger values, owing to the fact that they reproduced only the lower bathymetric points, whereas, in reality, the actual observed geoid is influenced by nearby masses. Therefore, the feature being studied will dictate whether we use the two- or the three-dimensional approach.

In the future, we intend to collect and study as many features as possible with various ages for the load and various ages of the lithosphere in order to deduce a relationship between flexural rigidity and age of the lithosphere. That study will first be carried systematically in the Pacific Ocean and then will be extended to all oceanic regions. This could be used as a method to derive the age of unknown loads.

Acknowledgment. This work was supported in part by contract SR 33852 with the Massachusetts

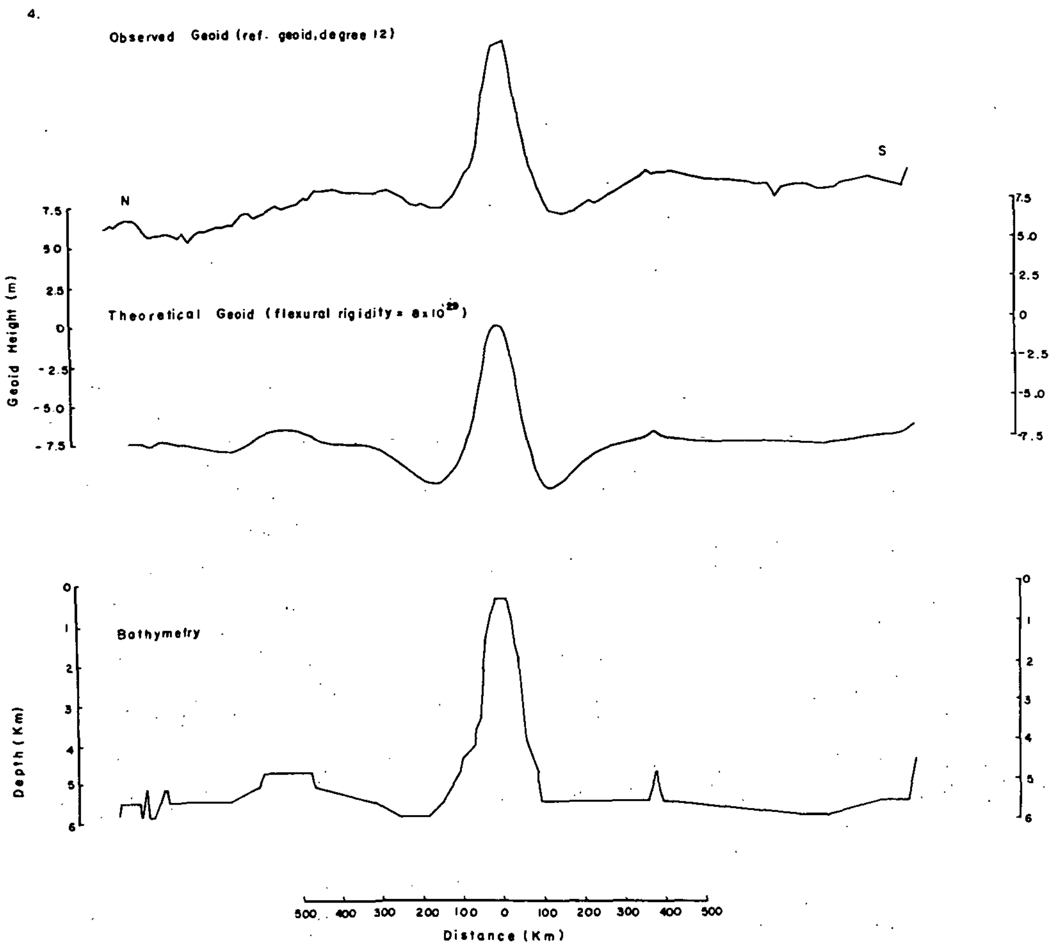

Fig. 5. The top profile represents the observed geoid with respect to a reference geoid of degree and order 12 in the Emperor Seasmount region; the intermediate profile is the predicted geoid calculated with a filter of flexural rigidity 8 x 10^{29} dyne-cm and convolved with the bathymetry represented on the bottom profile.

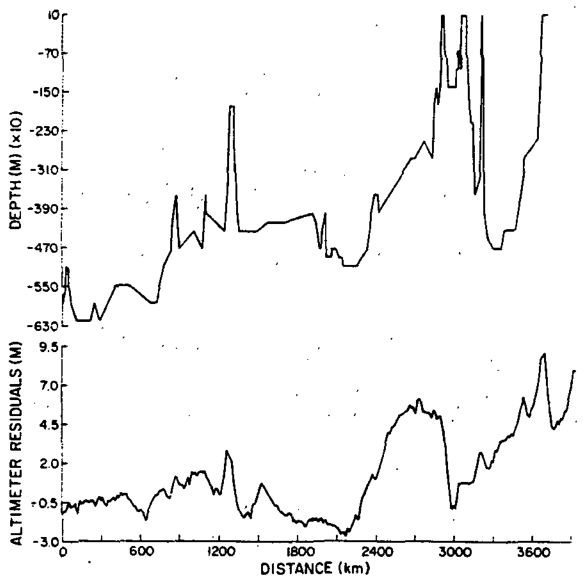

Fig. 6. The top profile represents the bathymetry in the Gilbert Islands region; the bottom profile represents the observed geoid with respect to a reference geoid of degree and order 16.

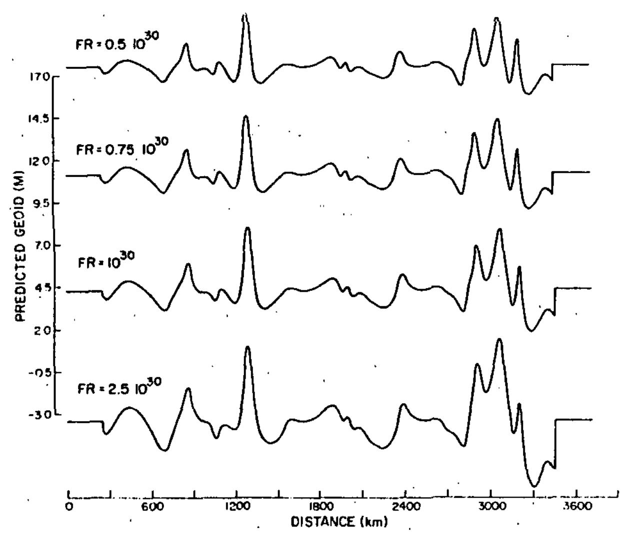

Fig. 7. The four profiles represent the predicted geoid in the Gilbert Islands region calculated with filters of different flexural rigidities: 0.5, 0.75, 1., and 2.5 (x 10^{30}) dyne-cm, respectively.

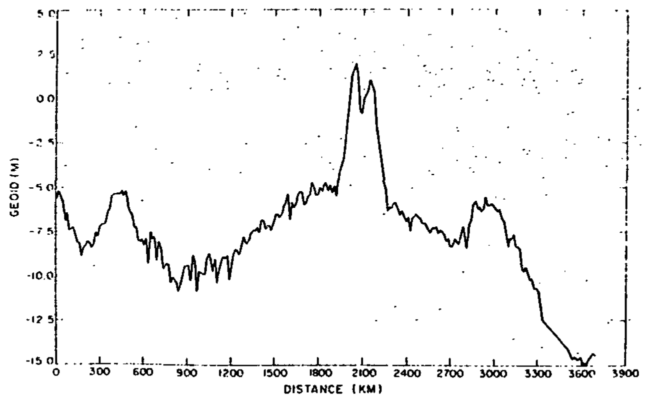

Fig. 8. Observed geoid with respect to a reference geoid of degree and order 16 in the Crozet region.

Institute of Technology and in part by contract F19628-78-C-0003 from the Air Force Geophysical Laboratory.

References

Chase, T.E., H.W. Menard, and J. Mammerickx, Bathymetry of the North Pacific, Scripps Institution of Oceanography and Institute of Marine Resources, 1970.

Clague, D.A., and R.D. Jarrard, Tertiary Pacific plate motion deduced from the Hawaiian-Emperor chain, Geol. Soc. Am. Bull., 84, 1135-1154, 1973.

Crough, S.T., Thermal model of oceanic lithosphere, Nature, 256, 388-390, 1975.

Larson, R.L., Late Jurassic and early Cretaceous evolution of the western central Pacific Ocean, Journ. Geomagn. Geochem., 28, 219-236, 1976.

McKenzie, D.P., Surface deformation, gravity anomalies and convection, Geophys. Journ. Roy. Astron. Soc., 48, 211-238, 1977.

McKenzie, D.P., J.M. Roberts, and N.O. Weiss, Convection in the earth's mantle: towards a numerical simulation, Journ. Fluid Mech., 62, 465-538, 1974.

McKenzie, D.P., and N.O. Weiss, Speculations on the thermal and tectonic history of the earth, Geophys. Journ. Roy. Astron. Soc., 42, 131-174, 1975.

McKenzie, D.P., and C. Bowin, The relationship between bathymetry and gravity in the Atlantic Ocean, Journ. Geophys. Res., 81, 1903-1915, 1976.

Schlich, R., Structure et age de l'Ocean Indien Occidental, Mem. Hors-Sene No. 6, Soc. Geol. France, Paris, 103, 1975.

Suyenaga, W., Earth deformation in response to surface loading, EOS, Trans. AGU, 58, 1231, 1977.

Walcott, R.I., Lithospheric flexure, analysis of gravity anomalies and the propagation of seamount chains. In "The Geophysics of the Pacific Ocean Basin and its Margin," ed. by G.H. Sutton, M.H. Manghnani, and R. Moberly, AGU Geophys. Mono. 19, Washington, D.C., pp. 431-438, 1976.

Watts, A.B., An analysis of isostasy in the world's oceans: Part 1 - Hawaiian-Emperor Seamount chain. Journ. Geophys. Res. (in press).

Watts, A.B., and J.R. Cochran, Gravity anomalies and flexure of the lithosphere along the Hawaiian-Emperor Seamount chain, Geophys. Journ. Roy. Astron. Soc., 38, 119-141, 1974.

Watts, A.B., J.R. Cochran, and G. Selzer, Gravity anomalies and flexure of the lithosphere: a three-dimensional study of the Great Meteor Seamount, Northeast Atlantic, Journ. Geophys. Res, 80, 1391-1398, 1975.

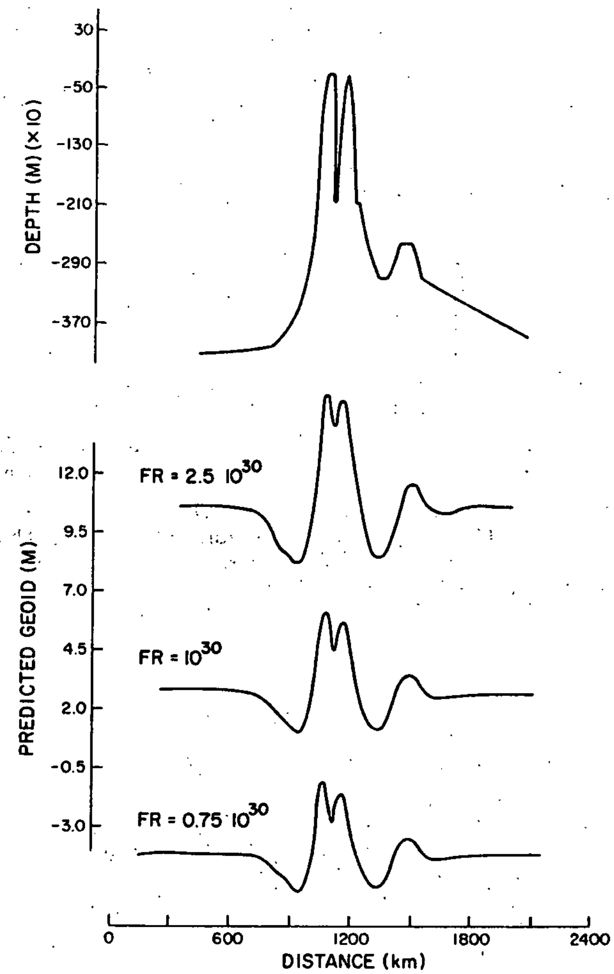

Fig. 9. The top profile is the bathymetry in the Crozet region; the three bottom profiles represent the predicted geoid calculated with filters of different flexural rigidities: 2.5, 1., and 0.75 (x 10^{30}) dyne-cm, respectively.